

Cite this: *Mater. Adv.*, 2026,
7, 2097

Properties of cyclic olefin-based photo-ROMP resins suitable for DLP 3D printing applications

Oleksandr Burtovyy,^a Kyle Cushman,^{id}^a Gerhard A. Meyer,^a Linda Zhang,^a
Leah Langsdorf,^{id}^a Alex Niemiec,^a Dan Gastaldo,^a Doug Skilskyj,^a
Krzysztof Skowerski^b and Larry F. Rhodes^{id}*^a

A series of cyclic olefin monomers, all based on derivatives of tetracyclododecene with different pendant groups, were evaluated as suitable candidates for photo-ROMP resins using a latent Ru precatalyst activated by a chlorinated thioxanthone (CPTX, 1-chloro-4-propoxythioxanthone) when exposed to purple light. Two monomers where the pendant group was hexyl or phenethyl are non-flammable and exhibited low volatility and odor. The thermomechanical properties of these two resins were determined after flood photo-curing. The high reactivity and excellent shelf-life photo-ROMP system augmented with a light absorber and base quencher allowed for production of DLP 3D printed parts. The thermomechanical properties of the 3D printed specimens were comparable to those of flood cured parts.

Received 12th November 2025,
Accepted 11th January 2026

DOI: 10.1039/d5ma01316j

rsc.li/materials-advances

Introduction

Additive manufacturing, more commonly known as 3D printing, allows practitioners the ability to create objects with an extreme degree of complexity. These objects can be tailored to individual needs providing a high degree of personalization. Examples include prosthetics, dental appliances, and earphones, to name a few.¹ Moreover, the quick turnaround of 3D printing enables customized formats that cannot be manufactured using traditional injection moulding approaches along with meeting cost of ownership requirements since the volume of these objects is generally relatively low.

There are several types of technologies available for 3D printing polymers including Selective Laser Sintering (SLS), Fused Deposition Modelling (FDM), Stereolithography (SLA) and Digital Light Processing (DLP), among others.² Of these, the first two rely on thermal processing either by fusing polymer particles (SLS) or extruding a thin polymer filament (FDM). The latter two are based on solvent-free, liquid UV-curable resins where either a laser “writes” the shape of successive layers of the part (SLA) or a light engine projects the shape of the part one layer at a time (DLP) onto a vat of the photopolymer resin.³

Generally, two types of polymerization mechanisms are operative upon light exposure of photosensitive resins in 3D printing: chain growth or step-growth.³ Chain growth mechanisms can be further categorized by free radical, cationic or anionic initiation and propagation.

Monomers that support the free-radical chain growth mechanism include (meth)acrylates, styrenics, or maleimides while epoxies or vinyl ethers can propagate by a cationic mechanism. Addition of a thiol functionality to olefins is an example of a step-growth mechanism that is initiated by photo-generation of a free radical.

Recently, there has been an increased interest in an alternative photopolymer resin class for the 3D printing space using photo-ROMP (ring opening metathesis polymerization) resins based on cyclic olefins. Photo-ROMP, originally disclosed in 1996,⁴ typically requires a photo-activated metal complex that can initiate the ROMP reaction. As pointed out by Leguizamon and co-workers, the metal complex can be either directly or indirectly activated by light, among other methods.⁵ Examples of direct photo-activation include ligand extrusion to create a reactive 14e complex^{6–8} or isomerization from a latent *cis* complex to a more reactive *trans* isomer.⁹ Examples of indirect photo-activation include excitation of photo-redox capable species,^{10,11} reaction with acid from an exposed photoacid generator (PAG),¹² and exposure of formulations incorporating photosensitizers (PS) with, optionally, a co-initiator (CoI).^{13,14}

Some of these photo-ROMP catalyst systems have been applied to SLA and DLP 3D printing techniques (Fig. 1a and b).^{13–16} The resin systems that have been disclosed rely chiefly on dicyclopentadiene (DCPD) as its major component due to its commercial availability, relatively low cost, and excellent properties of ROMP poly(dicyclopentadiene).^{17,18} However, to make DCPD (a solid at room temperature) amenable to 3D printing, prior investigators relied upon mixtures of DCPD with other reactive monomers such as ENB (ethylidene norbornene) to suppress the melting point of DCPD^{13,14,16} or heating the

^a Promerus, LLC, 225 W Bartges St, Akron, OH 44307, USA.

E-mail: larry.rhodes@promerus.com

^b Apeiron Synthesis, S.A., Duńska 9, Wrocław, 54-427, Poland

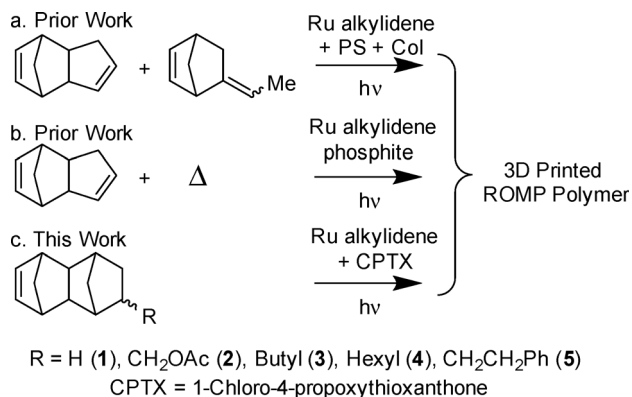


Fig. 1 3D printed ROMP polymers made using (a) Ru alkylidenes, photosensitizer (PS), and co-initiator (Col),¹³ (b) Ru alkylidene phosphite complexes,¹⁵ (c) Ru alkylidene plus CPTX.

DCPD¹⁵ to render it liquid increasing the complexity of the resin system. In addition, a small amount of solvent was typically required to dissolve the catalyst in the DCPD mixture.

Besides requiring a second monomer or heating to render DCPD liquid, there are other inherent properties of DCPD that make integration into 3D printing platform such as SLA or DLP problematic. Such platforms rely on an open vat of liquid photopolymer. Therefore resins based on monomers that are volatile, have an objectionable odour, a low odour threshold, and are flammable such as DCPD are not preferred.

Although modification of the printer platform can mitigate some of the issues associated with DCPD, a better approach would be to develop photo-ROMP resins based on monomers that do not suffer from DCPD's limitations. In this contribution, we detail our findings for a new class of photo-ROMP resins. These liquid resins are based on alternate cyclic olefin monomers that are not volatile, have no odour, and are not flammable (Fig. 1c). Their photo-polymerization reactivity, their shelf-life stability and their polymer properties for both flood exposure-cured films and DLP-printed specimens using a latent Ru alkylidene catalyst activated upon exposure by CPTX are discussed.

Results and discussion

Five new monomers were auditioned for suitability in 3D printing applications. Their structures, all derivatives of tetracyclododecene (monomer 1) with different pendant groups, are shown in Fig. 2. The monomers were evaluated regarding their state at room temperature, flammability (by flash point determination), volatility (by TGA) and odour, Table 1.

All the monomers evaluated were liquid at room temperature and are classified as combustible, not flammable, since their flash points are greater than 37.8 °C (100 °F). However, monomer 1 is unacceptable due to its high volatility (only 11.5% of the monomer remains after 6 h at 30 °C) and detectible odour. While monomers 2 and 3 are not flammable, they are not preferred due to their slight volatility and slight odour. Monomers 4 and 5 are ideal since they are liquid, not

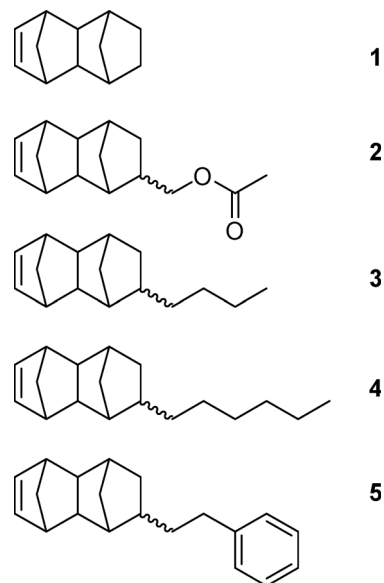


Fig. 2 Cyclic olefin monomers evaluated for 3D printing suitability.

Table 1 Evaluation results of monomers 1–5

Monomer	State at RT	Flash point (°C)	TGA ^a	Detectible odour
1	Liquid	102	11.5	Yes
2	Liquid	158	98.8	Slight
3	Liquid	141	96.4	Slight
4	Liquid	163	99.4	No
5	Liquid	185	99.9	No

^a WT% remaining after 6 h at 30 °C by TGA (Page S5).

flammable, not volatile, and do not emit a noticeable odour. These two monomers were chosen for further study.

In recent years, Promerus and Apeiron Synthesis have developed photo-initiated ROMP systems based on latent ruthenium carbide¹⁹ and alkylidene^{20–23} complexes activated upon exposure by PAGs and a chlorinated PS such as CPTX, respectively. In the case of the ruthenium carbides, the complexes were NHC (N-heterocyclic carbene) and CAAC (cyclic alkyl amino carbene) derivatives related to complexes originally reported by Heppert²⁴ and employed by Piers¹² in photo-ROMP chemistry initiated by a photoactivated PAG. In the case of the ruthenium alkylidenes, a unique photoactivated catalyst system was discovered that relies upon the generation of HCl from a chlorinated PS which activates a latent ruthenium alkylidene precatalyst **Ru-1** as reported by Sivaguru.²⁵ In this contribution we rely upon the same pathway to activate another latent Ru alkylidene precatalyst **Ru-2** (Fig. 3).²¹ It is noteworthy that both ruthenium precatalysts are soluble in neat monomer and do not require additional solvent.

A mould fabricated from a silicone piece sandwiched between two glass slides was filled with formulations of neat monomer 4 or 5 with **Ru-2** and CPTX (along with Irganox[®] 1076, and Irgafos[®] 168 to enhance oxidative stability) and



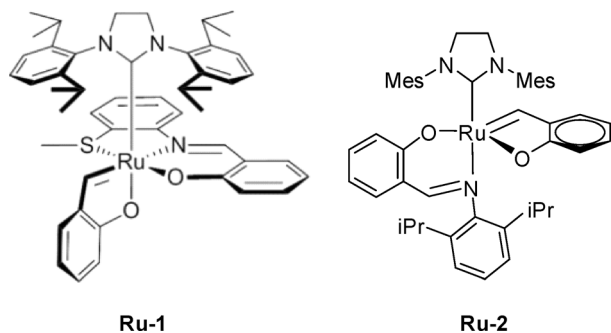


Fig. 3 Structures of **Ru-1** and **Ru-2** alkylidene precatalysts (Mes = 2,4,6-trimethylphenyl and iPr = isopropyl).

blanket exposed at 395 nm to make films of poly(**4**) and poly(**5**) (Page S6 and S12). Poly(**4**), after dissolution, exhibited backbone double bond protons centered at ~ 5.7 ppm in its ^1H NMR spectrum consistent with a ROMP polymer formation. No olefin peaks due to residual monomer were observed indicating conversion approaching 100% (Page S11). Poly(**4**) exhibited very high molecular weight as determined by GPC ($M_w = 611\,000$ and $M_n = 228\,000$, Page S10). Poly(**5**) was not soluble in common solvents such as chloroform, THF, toluene, or cyclohexane so no NMR or GPC data is extant. Nevertheless, a comparison of dynamic TGA data for monomer **5** with poly(**5**) is indicative of high polymerization conversion as there is no significant weight loss for poly(**5**) ($T_{d5} = 404$ °C) at the point where monomer **5** begins to evaporate ($T_{d5} = 190$ °C, Page S9). Similar behaviour is observed for monomer **4** and poly(**4**).

The cured films for poly(**4**) and poly(**5**) were subjected to several thermomechanical tests the results of which are presented in Table 2.

In general, poly(**5**) appears to be stiffer than poly(**4**); its tensile modulus is about double that of poly(**4**). As might be expected for a more rigid material, the elongation to break for poly(**5**) is lower than poly(**4**). The impact strength of poly(**4**) is extremely high, while in keeping with a stiffer material, the impact strength of poly(**5**) is much lower. Both poly(**4**) and poly(**5**) exhibit high T_g s based on the $\tan \delta$ peak from their DMA curves. In accordance with its higher T_g , the heat deflection temperature (HDT at 0.455 MPa) of poly(**5**) is about 20 °C higher than poly(**4**).

It is instructive to compare typical thermomechanical property data for ROMP poly(DCPD) to that found for poly(**4**) and poly(**5**). According to a recent review, the tensile modulus values for thermally-cured ROMP poly(DCPD) range from 1.6 to 2.0 GPa and ETB can be as high as 100%.²⁶ Park, *et al.* reported that poly(DPCD) made using a thermal ruthenium system yielded notched Izod impacts of about 500 to 650 J m^{-1} depending on the cure temperature.²⁷ Depending on the extent of crosslinking, poly(DPCD) exhibits T_g s from 140 to 165 °C.²⁶ However, for the photo-cured poly(DCPD/ENB 95/5) resins, the tensile modulus was substantially less (between 500–700 MPa, depending on catalyst) while the T_g remained similar (between 155 °C and 165 °C by DMA) after thermal postcure.¹³

Note that poly(**4**) and poly(**5**) having only a single double bond for each monomer repeat unit are not susceptible to

Table 2 Thermomechanical properties of flood photo-cured specimens (10 J cm^{-2} at 395 nm) of poly(**4**) and poly(**5**). (10 K:1:10:49:10 molar ratio of monomer:**Ru-2**:CPTX:Irganox[®] 1076:Irgafos[®] 168)

Monomer	Modulus (Gpa)	ETB (%)	Impact (J m^{-1})	T_g (°C)	HDT (°C)
4	0.97 ± 0.03	218 ± 20	805 ± 63	128 ± 1	78 ± 1
5	2.3 ± 0.2	147 ± 13	42 ± 5.8	130.7 ± 3.0	91

crosslinking as observed for DCPD. While poly(**5**) is not soluble in common solvents (perhaps due to extremely high molecular weight), the storage modulus for both poly(**4**) and poly(**5**) approaches zero above T_g consistent with very limited crosslinking (Page S13). Despite the lack of crosslinking, it is apparent from the data in Table 2 that the critical thermomechanical properties of poly(**4**) and poly(**5**) made using our photo-ROMP system are comparable to poly(DCPD) wherein poly(**5**) provides a more rigid material while poly(**4**) is a softer material. The thermomechanical properties of these photo-ROMP materials are likely enhanced by their very high molecular weights.

Prior to embarking on 3D printing experiments, we examined the behaviour of the photo-ROMP system using **Ru-2** for both monomers **4** and **5** using photo-DSC. Data regarding the dose and speed of the reaction from photo-DSC can inform parameters for 3D printing objects where not only the dose is important but so is the exposure time per layer.²⁸

The photo-DSC behaviour in Fig. 4 shows that monomer **4** reacts faster than **5** at 30 °C. Within ~ 4 s after exposure, monomer **4** reaches peak exotherm, while monomer **5** requires ~ 11 s and the exotherm is much broader. At higher temperature, the speed of reaction for monomer **5** is increased as would be expected. At 60 °C, monomer **5** reaches maximum exotherm within ~ 3 s after exposure and is much sharper than at 30 °C. The slower reactivity of monomer **5** may be related to the more sterically bulky pendant group. The photo-ROMP resin based on monomer **4** was evaluated further for its suitability in DLP 3D printing since a resin with faster reactivity near room temperature would be more readily integrated into existing 3D printers and thus would be more widely acceptable to the 3D printing community (Fig. 4).

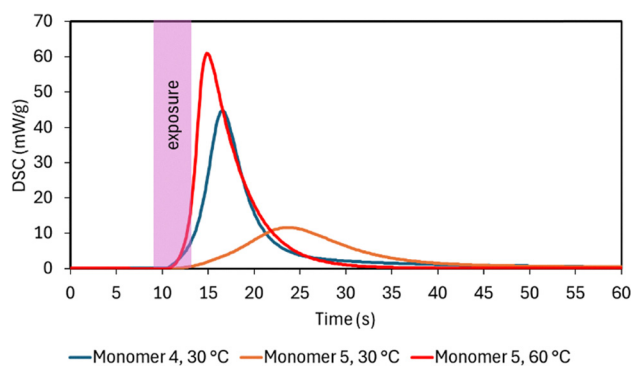


Fig. 4 DSC exotherms after 1 J cm^{-2} exposure (395 nm) at 30 °C for both monomer **4** and **5** and DSC exotherm for monomer **5** at 60 °C. (10 K:1:10:49:10 molar ratio of monomer:**Ru-2**:CPTX:Irganox[®] 1076:Irgafos[®] 168).

In 3D printing methods such as DLP or SLA that require liquid photo-active resin, two figures of merit are important: shelf-life and vat-life stability (also known as working or pot-life). Good shelf- and vat-life is defined as stable viscosity and reactivity over time. In Fig. 5, viscosity and heat of reaction (by photo-DSC) for a formulation of monomer **4**, **Ru-2** and CPTX stored at room temperature is presented. These data show little change in either parameter over 20 days indicating excellent shelf-life stability.

Next, our attention turned to printing objects using the monomer **4**, **Ru-2**, and CPTX resin composition. An off-the-shelf Flashforge Hunter DLP printer was used that had been modified to print under a nitrogen atmosphere (Page S8). Our previous study indicated that oxygen quenches the photo-excited state of CPTX thus interrupting the activation of the ruthenium precatalyst.²⁵ Despite these precautions, after an overnight printing cycle the resin in the vat of the printer gelled.

Two potential root causes for premature gelation were considered. One root cause could be light scattering during exposure causing a loss in resolution. To counteract this issue, we added a light absorber to the resin. Such additives are known to enhance resolution.²⁹ We found that 2,5-bis(5-*tert*-butyl-benzoxazol-2-yl)thiophene (bTBBT) not only can serve as a light absorber,^{29–31} it is completely compatible with the ROMP chemistry initiated by our photo-ROMP catalyst. Another root cause might be migration of HCl throughout the resin from CPTX degradation beyond the exposed area. Chloride anion has been postulated as the necessary activator of the latent ruthenium precatalyst in the current photo-ROMP system.²⁵ Similar acid migration issues in chemically amplified photoresists are known to reduce resolution resulting in blur and increase in line edge roughness. Such problems have been solved by addition of a base quencher to the resin.³² To mitigate this possible issue in our resins, we added a nitrogen base, 4-dimethylaminopyridine (DMAP) (Page S16).

We were pleased to discover that a photo-ROMP resin consisting of monomer **4**, **Ru-2**, CPTX, bTBBT, and DMAP could successfully be printed using our DLP printer into a myriad of shapes (Fig. 6 and Pages S19–S20).

Once the vat-life of the new resin formulation was shown to be sufficiently long (over 20 h demonstrated) to enable 3D

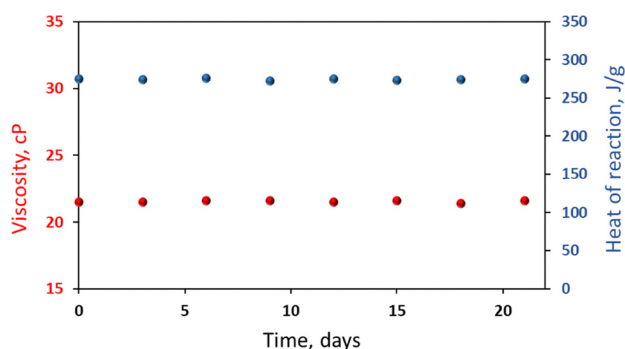


Fig. 5 Viscosity and reaction enthalpy of monomer **4** formulated with **Ru-2** and CPTX stored at room temperature over time. (10 K:1:10:49:10 molar ratio of monomer:**Ru-2**:CPTX:Irganox[®] 1076: Irgafos[®] 168).

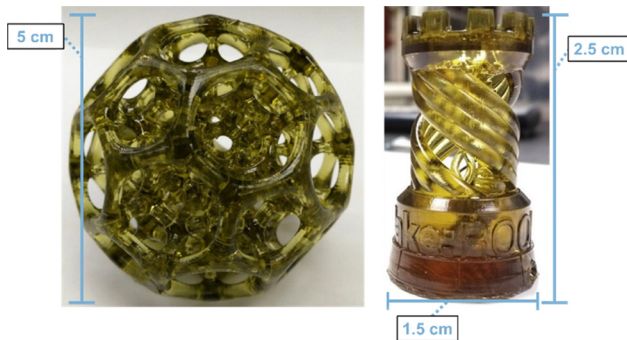


Fig. 6 Examples of objects printed using resin formulation consisting of monomer **4**, **Ru-2**, CPTX, bTBBT, DMAP, Irganox[®] 1076, and Irgafos[®] 168.

Table 3 Thermomechanical properties of monomer **4** formulation (10 K:1:40:0.1:0.01:49:10 molar ratio of monomer:**Ru-2**:CPTX:DMAP:bTBBT:Irganox[®] 1076:Irgafos[®] 168) after flood curing, 3D printing and 3D printing plus post-printing UV flood exposure

Property	Flood exposed	Printed ^a	Printed + UV postcured ^b
Modulus (GPa)	0.9 ± 0.03	0.2 ± 0.03	0.8 ± 0.1
ETB (%)	220 ± 25	240 ± 40	190 ± 30
HDT (°C)	81 ± 2	65 ± 5	81 ± 2
Impact (J m ⁻¹)	600 ± 4	700 ± 20	100 ± 7

^a 50 μm layer, 8 mW cm⁻², 20–30 s layer⁻¹. ^b 20 min exposure, 25 mW cm⁻², Hg lamp.

printing of objects, the question became whether the suite of excellent thermomechanical properties demonstrated for flood exposed parts would translate to 3D printed test specimens. To answer this question full formulations of **4**, **Ru-2**, CPTX, DMAP, bTBBT, antioxidant (Irganox[®] 1076), and synergist (Irgafos[®] 168) were flood exposure cured as a baseline as well as 3D printed, followed by post printing UV flood curing.

From the data in Table 3, it is evident that most of the properties of the flood exposed formulation are very similar to those of the 3D printed specimen after UV post-curing. UV post-curing is typically employed in 3D printing to ensure complete conversion of the resin in the part and thus improve the properties. The properties of the printed part without UV post-curing are skewed to that of a softer material (lower modulus and lower HDT) as expected for a somewhat lower conversion which is remedied by UV post-curing.

The only property that is not improved in the post-cured 3D printed specimen compared to the flood exposed specimen is the impact resistance. Lower impact resistance may be due to the anisotropic nature of 3D printed specimens. Nevertheless, the impact value obtained for the UV post-cured parts based on monomer **4** is higher than many vat photopolymer resins.³³

Conclusions

A series of cyclic olefins with different pendant groups were evaluated as monomers for a photo-ROMP system based on a latent ruthenium precatalyst activated by CPTX when exposed



to purple light. When the pendant group is either hexyl (monomer 4) or phenethyl (monomer 5), the monomer is not flammable, not volatile and has no detectable odor. The thermomechanical properties of resins based on both monomers were determined after flood exposure curing. Poly(4) is a softer, less rigid material compared to poly(5) and, as such, exhibits an extremely high impact resistance.

Photo-DSC measurements show that monomer 4 reacts quicker than 5 near room temperature and is therefore more suitable for widespread adoption in the 3D printing ecosystem where most printing is done at room temperature. Formulations of monomer 4 exhibit an exemplary shelf life of over 20 days at room temperature. When light absorber and base quencher additives are used, the vat life of these resins is sufficient for printing of 3D objects.

Finally, 3D printed specimens based on monomer 4 after post-printing UV curing showed thermomechanical properties very similar to those of flood exposed specimens with the exception of impact resistance. Nevertheless, the value obtained should be considered excellent compared to other 3D printing resins.

Oleksandr Burtovyy: resources, conceptualization. Data curation. Kyle Cushman: resources, data curation. Linda Zhang: resources. Leah Langsdorf: supervision. Alex Niemiec: resources. Dan Gastaldo: resources. Gerhard Meyer: resources, data curation. Doug Skilskyj: resources. Krzysztof Skowerski: resources, conceptualization. Larry Rhodes: writing, reviewing and editing, conceptualization.

Conflicts of interest

There are no conflicts to declare.

Data availability

The data supporting this article have been included as part of the supplementary information (SI). Supplementary information: experimental details, supporting characterization data. See DOI: <https://doi.org/10.1039/d5ma01316j>.

Acknowledgements

We thank Hugh Burgoon for the NMR and Jessica Koester and Jennifer Thoresen for the GPC measurement.

References

- https://formlabs.com/blog/25-unexpected-3d-printing-use-cases/?srsltid=AfmBOor7YrIpVpCCn_y4quUyqIQ1MguXV0LXgy93cEXsqPvteUw2bj0, accessed Nov., 2025.
- B. Narupai and A. Nelson, 100th Anniversary of Macromolecular Science Viewpoint: Macromolecular Materials for Additive Manufacturing, *ACS Macro Lett.*, 2020, **9**, 627–638.
- A. Bagheri and J. Jin, Photopolymerization in 3D Printing, *ACS Appl. Polym. Mater.*, 2019, **1**, 593–611.
- P. A. van der Schaaf, A. Hafner and A. Mühlebach, Photo-induced Ring Opening Metathesis Polymerization (PROMP) with Photochemically Generated Schrock Type Catalysts, *Angew. Chem., Int. Ed. Engl.*, 1996, **35**(16), 1845–1847.
- A. J. Greenlee, R. A. Weitekamp, J. C. Foster and S. C. Leguizamon, PhotoROMP: The Future Is Bright, *ACS Catal.*, 2024, **14**, 6217–6227.
- R. A. Weitekamp, H. A. Atwater and R. H. Grubbs, Photolithographic Olefin Metathesis Polymerization, *J. Am. Chem. Soc.*, 2013, **135**, 16817–16820.
- O. Eivgi, S. Guidone, A. Frenklah, S. Kozuch, I. Goldberg and N. G. Lemcoff, Photoactivation of Ruthenium Phosphite Complexes for Olefin Metathesis, *ACS Catal.*, 2018, **8**, 6413–6418.
- A. Vaisman, Y. Vidavsky, M. Baranov, A. Lehrer, J. H. Baraban and N. G. Lemcoff, Latency for All: Enabling Latency of Hoveyda–Grubbs Second-Generation Catalysts by Adding Phosphite Ligands, *J. Am. Chem. Soc.*, 2024, **146**, 73–78.
- N. B. Nechmad, V. Kobernik, N. Tarannam, R. Phatake, O. Eivgi, S. Kozuch and N. G. Lemcoff, Reactivity and Selectivity in Ruthenium Sulfur-Chelated Diiodo Catalysts, *Angew. Chem.*, 2021, **133**, 6442–6446.
- C. Theunissen, M. A. Ashley and T. Ravis, Visible-Light-Controlled Ruthenium-Catalyzed Olefin Metathesis, *J. Am. Chem. Soc.*, 2019, **141**, 6791–6796.
- J. V. Musso, P. Gebel, V. Gramm, W. Frey and M. R. Buchmeiser, Tungsten Oxo and Tungsten Imido Alkylidene N-Heterocyclic Carbene Complexes for the Visible-Light-Induced Ring-Opening Metathesis Polymerization of Dicyclopentadiene, *Macromolecules*, 2023, **56**, 2878–2888; B. K. Keitz and R. H. Grubbs, A Tandem Approach to Photoactivated Olefin Metathesis: Combining a Photoacid Generator with an Acid Activated Catalyst, *J. Am. Chem. Soc.*, 2009, **131**(6), 2038–2039.
- A. Y. Khalimon, E. M. Leitao and W. E. Piers, Photogeneration of a Phosphonium Alkylidene Olefin Metathesis Catalyst, *Organometallics*, 2012, **31**(15), 5634–5637.
- S. C. Leguizamon, N. T. Monk, M. T. Hochrein, E. M. Zapien, A. Yoon, J. C. Foster and L. N. Appelhans, Photoinitiated Olefin Metathesis and Stereolithographic Printing of Polydicyclopentadiene, *Macromolecules*, 2022, **55**, 8273–8282.
- J. C. Foster, A. W. Cook, N. T. Monk, B. H. Jones, L. N. Appelhans, E. M. Redline and S. C. Leguizamon, Continuous Additive Manufacturing using Olefin Metathesis, *Adv. Sci.*, 2022, **9**, 2200770.
- O. Eivgi, A. Vaisman, N. B. Nechmad, M. Baranov and N. G. Lemcoff, Latent Ruthenium Benzylidene Phosphite Complexes for Visible-Light-Induced Olefin Metathesis, *ACS Catal.*, 2020, **10**, 2033–2038.
- S. C. Leguizamon, K. Lyons, N. T. Monk, M. T. Hochrein, B. H. Jones and J. C. Foster, Additive Manufacturing of Degradable Materials via Ring-Opening Metathesis Polymerization (ROMP), *ACS Appl. Mater. Interfaces*, 2022, **14**, 51301–51306.
- <https://www.slideshare.net/slideshow/dcpdtelene-rim-polymer-pdf/257470508#6>, accessed Nov., 2025.



- 18 <https://www.lookpolymers.com/pdf/Lubrizol-Telene-1650-ABK-Dicyclopentadiene-DCPD.pdf>, accessed Nov., 2025.
- 19 R. Gawin, O. Burtovyy and L. F. Rhodes, *Organoruthenium Carbide Complexes as Precatalysts for Olefin Metathesis*, US11291983, 2022.
- 20 O. Burtovyy, *Stable Mass Polymerizable Polycycloolefin Compositions as 3D Printing Materials and a Method of Fabrication Thereof*, US12037431, 2024.
- 21 K. Skowerski, J. Pomorskie, M. Chwalba, A. Gawin, R. Gawin and P. Krajczy, *Organoruthenium Complexes as Precatalysts for Olefin Metathesis*, US11939410, 2024.
- 22 O. Burtovyy, *Long Shelf Life Stable Photoactive Mass Polymerizable Polycycloolefin Compositions as Optical Materials*, US11535702, 2022.
- 23 M. Chwalba, K. Skowerski, J. Pomorskie and K. Kurbach, *Long Shelf Life Stable Organoruthenium Complexes as (Pre)-Catalysts for Olefin Metathesis*, US20240150384, 2024.
- 24 R. G. Carlson, M. A. Gile, J. A. Heppert, M. H. Mason, D. R. Powell, D. V. Velde and J. M. Vilain, The Metathesis-Facilitated Synthesis of Terminal Ruthenium Carbide Complexes: A Unique Carbon Atom Transfer Reaction, *J. Am. Chem. Soc.*, 2002, **124**, 1580–1581.
- 25 K. Manal, S. Jockusch, O. Burtovyy, L. Zhang, L. Langsdorf, A. Niemiec, D. Gastaldo, D. Skilskyj, M. Chwalba, L. F. Rhodes and J. Sivaguru, Ruthenium Catalyzed PhotoROMP Activated by a Chlorine Functional Thioxanthone (CPTX), *J. Photochem. Photobiol., A*, 2026, **472**, 116728–116734.
- 26 S. Kovačič and C. Slugovc, Ring-opening Metathesis Polymerisation Derived Poly(dicyclopentadiene) based Materials, *Mater. Chem. Front.*, 2020, **4**, 2235–2255.
- 27 H.-S. Park, P.-S. Shin, J.-H. Kim, Y.-M. Baek, D.-J. Kwon, W.-I. Lee, K. L. DeVries and J.-M. Park, Evaluation of Interfacial and Mechanical Properties of Glass Fiber/Poly-Dicyclopentadiene Composites with Different Post Curing at Ambient and Low Temperatures, *Fibers Polym.*, 2018, **19**(9), 1989–1996.
- 28 J. Bachmann, E. Gleis, S. Schmölder, G. Fruhmann and O. Hinrichsen, Photo-DSC Method for Liquid Samples Used in Vat Photopolymerization, *Anal. Chim. Acta*, 2021, **1153**, 338268.
- 29 C. Kolb, N. Lindemann, H. Wolter and G. SEXTL, 3D-Printing of Highly Translucent ORMOCER[®]-based Resin Using Light Absorber for High Dimensional Accuracy, *J. Appl. Polym. Sci.*, 2021, **138**, e49691.
- 30 R. Borayek, P. Zhang, H. J. Willy, M. Zedan, J. Zhu and J. Ding, Programmable, UV-Printable Dielectric Elastomers Actuate at Low Voltage without Prestretch and Supporting Frames, *ACS Appl. Electron. Mater.*, 2020, **2**, 4042–4053.
- 31 R. J. Viereckl, M. Gould, V. Petry, R. Dodd, X. Marguerettaz and S. D. Roches, <https://uvebtech.com/articles/2018/formulating-for-3d-printing-constraints-and-components-for-stereolithography/>, accessed Nov., 2025.
- 32 C. L. Henderson, in *Polymer Science: A Comprehensive Reference Photoresists and Advanced Patterning*, ed., K. Matyjaszewski, M. Möller, Elsevier, 2012, ch. 8.03, pp. 37–76.
- 33 <https://www.liqcreate.com/supportarticles/the-tough-3d-printing-resin-sla-dlp-lcd-msla/>, accessed Nov. 2025.

